Key Points:
- Analyzed populations of *Neogloboquadrina* foraminifera show no size-dependent offsets in B/Ca and significant correlations with carbonate system variables
- B/Ca of individual *G. bulloides* analyzed by LA-ICP-MS indicates that local cryptic species have significant B/Ca offsets
- Divergent geochemistry of cryptic species calls into question the use of traditional species classification for B/Ca analysis

Correspondence to:
E. B. Osborne,
emily.osborne@noaa.gov

A Sediment Trap Evaluation of B/Ca as a Carbonate System Proxy in Asymbiotic and Nondinoflagellate Hosting Planktonic Foraminifera

Emily B. Osborne[1,2] [ID], **Natalie E. Umling[3]** [ID], **Michael Bizimis[4]** [ID], **Wayne Buckley[5]** [ID], **Aleksey Sadekov[6]**, **Eric Tappa[4]** [ID], **Brittney Marshall[7]**, **Leslie R. Sautter[8]**, and **Robert C. Thunell[4,9]** [ID]

[1]Ocean Acidification Program, National Oceanic and Atmospheric Administration, Silver Spring, MD, USA, [2]Cooperative Program for the Advancement of Earth System Science, University Corporation for Atmospheric Research, Boulder, CO, USA, [3]Department of Earth and Planetary Sciences, American Museum of Natural History, New York, NY, USA, [4]School of the Earth, Ocean and Environment, University of South Carolina, Columbia, SC, USA, [5]Jacobs JETS, NASA Johnson Space Center, Houston, TX, USA, [6]Engineering and Mathematical Sciences, Oceans Graduate School, The University of Western Australia, Perth, WA, Australia, [7]BHP Petroleum, Houston, TX, USA, [8]Department of Geology and Environmental Geosciences, College of Charleston, Charleston, SC, USA, [9]Deceased 30 July 2018

Abstract The ratio of boron to calcium (B/Ca) in a subset of foraminifera has been shown to covary with seawater carbonate chemistry, making this geochemical signature a promising proxy for carbon cycle science. Some studies suggest complications with the B/Ca proxy in photosymbiont-bearing planktonic foraminifera, while relatively few studies have investigated B/Ca in species that lack large dinoflagellate symbionts. For the first time, we use a sediment trap time series to evaluate B/Ca of subtropical and subpolar planktonic foraminifera species that are asymbiotic (*Globigerina bulloides* and *Neogloboquadrina incompta*) and a species that hosts small intrashell photosymbionts (*Neogloboquadrina dutertrei*). We find that B/Ca measurements across size fractions indicate overall little to no size-dependent uptake of boron that has previously been reported in some symbiont-bearing foraminifera. *Neogloboquadrina incompta* and *N. dutertrei* B/Ca are strongly correlated with calcite saturation, pH, and carbonate ion concentration, which is in good agreement with the limited number of published core top results. While *G. bulloides* B/Ca trends with seasonal fluctuations in carbonate chemistry, during discrete periods considerable B/Ca offsets occur when a cryptic *G. bulloides* species is known to be seasonally present within the region. We confirm presence and significant B/Ca offset between cryptic species by individual LA-ICP-MS analyses. This finding calls into question the use of traditional morphological classification to lump what might be genetically distinct species for geochemical analyses. Our overall results highlight the utility of *G. bulloides*, *N. incompta*, and *N. dutertrei* B/Ca while bringing to light new considerations regarding divergent geochemistry of cryptic species.

1. Introduction

Understanding past carbon cycling in the oceans is important to identifying processes that have influenced climate in the past and understanding how climate may vary in the future. To address this question, considerable effort has gone into developing paleoproxies and applying them to sediment records to reconstruct past conditions of the marine carbonate system. The fossil shells of planktonic foraminifera that are widely distributed and well preserved in marine sediments provide an excellent tool for investigating past sea surface chemistry via proxy methods. The concentration of boron in the calcium carbonate shells produced by foraminifera, or the boron to calcium ratio (B/Ca), is one such proxy that has been proposed to covary with marine carbonate system variables (e.g., Allen et al., 2011; Foster, 2008; Ni et al., 2007; Yu et al., 2007).

In seawater, dissolved boron exists primarily as a mixture of two aqueous forms: boric acid (B $(OH)_3$) and borate (B $(OH)_4^-$). The speciation of boron in seawater is highly pH dependent, with borate concentrations dominating under elevated pH conditions. Studies have shown that the boron isotopic composition of marine carbonates is similar to that of the isotopic composition of borate in seawater, suggesting that borate is the boron species preferentially incorporated into the crystal lattice of marine carbonates (Hemming & Hanson, 1992; Sanyal et al., 1996). Foraminiferal culture results have confirmed that only 3–8% of the

total boron incorporated into the cultured shells of the planktonic foraminifera *Orbulina universa* was from boric acid (Allen et al., 2011). Taken together, this suggests that the concentration of boron measured in foraminifera represents the concentration of borate in sweater, both of which are positively correlated pH of seawater.

Hemming and Hanson (1992) and Yu et al. (2007) proposed an equilibrium reaction (equation (1)) and partition coefficient (K_D; equation (2)), respectively, to describe the theoretical incorporation of boron into marine calcites relative to ambient seawater composition. Studies that applied this theoretical framework have arrived at mixed results, including studies that found a mixture of strong (positive and negative) correlations between K_D and temperature (Foster, 2008; Yu et al., 2007), [CO_3^{2-}] (Foster, 2008) and growth rate (Ni et al., 2007). Resulting inconsistencies point to an incomplete understanding of how carbonate system parameters interact with boron incorporation into the calcite lattice which poses a looming uncertainty on the application of K_D (Allen et al., 2012). Many studies have turned to empirical calibrations, which have been applied to many other foraminifera-based proxies including the widely used Mg/Ca-temperature proxy. These empirical relationships are useful because foraminiferal calcite does not form in complete chemical equilibrium with seawater as evidenced by species-specific offsets and interactions with symbiotic organisms (e.g., Allen et al., 2011).

$$CaCO_3 + B(OH)_4^- \leftrightarrow CaHBO_3 + HCO_3^- + H_2O \tag{1}$$
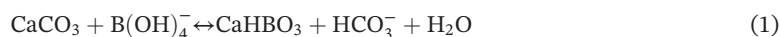
$$K_D = \frac{B/Ca_{calcite}}{\left[B(OH)_4^-\right]/\left[HCO_3^-\right]_{seawater}} \tag{2}$$

Developing the B/Ca carbonate chemistry proxy, particularly for planktonic foraminifera, has been the focus of several core top (Henehan et al., 2015; Foster et al., 2008; Ni et al., 2007; Quintana Krupinski et al., 2017; Yu et al., 2007), culture (Allen et al., 2011, 2012; Haynes et al., 2017; Henehan et al., 2015; Holland et al., 2017; Howes et al., 2017), and sediment trap studies (Babila et al., 2014; Salmon et al., 2016). In particular, these studies have for the most part have focused on developing a B/Ca carbonate chemistry proxy from large tropical and subtropical planktonic foraminifera species that harbor photosynthetic symbionts. Proxy records from symbiont-bearing species are advantageous because these species are confined to the surface ocean thereby reflecting processes occurring at the ocean-atmosphere interface, whereas many symbiont-barren species are found at greater depths within the upper water column and often near the thermocline.

Early core top studies suggested a strong species-specific response of B/Ca measured in planktonic foraminifera controlled by ambient carbonate system variables (pH and [CO_3^{2-}]) and growth rate, when temperature is accounted for (Foster, 2008; Ni et al., 2007; Yu et al., 2007). Later results from culture experiments using three tropical spinose species of planktonic foraminifera (*Orbulina universa*, *Globigerinoides sacculifer* and *Globigerinoides ruber* (pink)) found that B/Ca increased with increasing in pH and decreases with increasing dissolved inorganic carbon (DIC) and that temperature actually plays a negligible role in boron incorporation (Allen et al., 2011, 2012). Despite positive culture results for *G. ruber* (pink), a compilation of culture and globally distributed plankton tow, sediment trap, and core top B/Ca data for *G. ruber* (white) shows potential complicating effects (Henehan et al., 2015). Rather than documenting a significant relationship between B/Ca and carbonate chemistry, *G. ruber* B/Ca has shown moderately strong correlations with nutrient concentration ([PO_4^{3-}]; $R^2 = 0.33$) and salinity ($R^2 = 0.40$) (Henehan et al., 2015). Similarly, a sediment trap evaluation of *G. ruber* (white) B/Ca ratios from the oligotrophic North Atlantic found a considerable seasonal signal of 20–30 μmol/mol, despite location of the sediment trap in a region with little to no seasonal change in carbonate chemistry, suggesting that the *G. ruber* B/Ca variability was not due to changing seawater pH (Babila et al., 2014). An additional sediment trap study using this same time series reported on *O. universa*, *G. ruber* (pink), and *Globorotalia truncatulinoides* B/Ca and found similar size fraction offsets for *G. ruber* (pink) as well as a significant relationship between B/Ca with shell thickness (measured by area density; Salmon et al., 2016), which has been cited as being a highly significant [CO_3^{2-}] proxy (Marshall et al., 2013; Osborne et al., 2016; Osborne et al., 2019). It is important to note that Salmon et al. (2016) interestingly did not find a strong correlation with depth-specific [CO_3^{2-}], despite the inherent relationship between this carbonate variable and foraminiferal shell area density.

One possibility is that these complicating effects reported by previous studies are caused by modification of the foraminifera microenvironment by photosynthetic dinoflagellate symbionts. B/Ca ratios from different size fractions might be the result of increasing photosynthetic activity of dinoflagellate symbionts hosted on *G. ruber* spines that elevate ambient pH in the microenvironment around the foraminifera, thereby elevating B/Ca ratios in larger individuals that host a greater number of symbionts (Babila et al., 2014). Similarly, studies of calcite chemical banding in *O. universa* (Allen et al., 2011; Branson et al., 2015) and dissolution-induced decreases in core top *G. sacculifer* and *G. ruber* B/Ca ratios indicate that B incorporation into dinoflagellate symbiont-bearing species is heterogeneous (Dai et al., 2016). Subsequent culture studies of *Orbulina universa* have further shown the influence of photosynthetic activity of symbionts on the microenvironment of the foraminifera represented as banded day-night B/Ca signatures (Haynes et al., 2017; Holland et al., 2017). While complicating, such banding has been observed in many planktonic species (spinose and nonspinose) for B/Ca as well as other geochemical proxies such as Mg/Ca; these proxies have still successfully developed and applied to downcore records (e.g., Eggins et al., 2004; Fehrenbacher et al., 2015; Haynes et al., 2017).

It is important to also note that offsets in other trace metal ratios have also already been documented in varying size classes of planktonic foraminifera (Elderfield et al., 2002; Ni et al., 2007). An alternate hypothesis for the observed offsets in B/Ca ratios across different foraminiferal size fractions could be due to varying growth rates of different size individuals that may alter the rate of trace element incorporation (Babila et al., 2014). Inorganic calcite precipitation experiments have shown that calcification rate and calcite growth may influence boron incorporation and suggest that, in general, larger individuals incorporate more boron than smaller individuals (Ruiz-Agudo et al., 2012; Babila et al., 2014).

Studying asymbiotic and geochemically homogenous foraminifera presents an opportunity to further evaluate and develop the planktonic foraminifera B/Ca carbonate chemistry proxy. Evaluating such species eliminates the variables, including microhabitat modification by photosynthetic symbionts and shell geochemical heterogeneity, allowing for perhaps a clearer framework understanding boron incorporation into foraminiferal shells. Results from Pacific core top samples show a strong positive correlation of B/Ca from the asymbiotic planktonic foraminifera (*Neogloboquadrina incompta Globigerina bulloides*) B/Ca with the calcite saturation state of seawater ($\Omega_{calcite}$) and other carbonate system parameters (Quintana Krupinski et al., 2017). Likewise, results from dissolution studies of B/Ca from two planktonic foraminifera species that harbor small intrashell algal symbionts (*Neogloboquadrina dutertrei* and *Pulleniatina obliquiloculata*) suggest that there is a homogeneous distribution of boron in nondinoflagellate symbiont-bearing foraminiferal shells (Dai et al., 2016; Gastrich, 1987). Dissolution studies indirectly may suggest that shell heterogeneity is nonexistent in these species; citing this is one possible signal of a microenvironment/symbiont control on B/Ca (Holland et al., 2017).

Here, we seek to determine whether B/Ca ratios in asymbiotic and intrashell symbiont-bearing species from a Pacific sediment trap time series vary across size fractions and correlate with ambient carbonate chemistry variables. Our research focuses on the subpolar to polar asymbiotic species *N. incompta* (nonspinose) and bacterial (*Synechococcus*) endobiont-hosting *G. bulloides* (spinose), along with a nonspinose species that hosts small algal (chrysophyte) endobionts, *N. dutertrei* (Bird et al., 2017). Our sediment trap analysis will be the first for these species and will supplement existing core top results for *G. bulloides* (Quintana Krupinski et al., 2017; Yu et al., 2007), *N. incompta* (Quintana Krupinski et al., 2017) and *N. dutertrei* (Foster, 2008).

2. Materials and Methods
2.1. Oceanographic Setting

This study uses planktonic foraminifera shells and water column data collected off the California Margin in the Santa Barbara Basin (SBB) where the University of South Carolina has maintained a sediment trap mooring since 1993. There are north and south bounding continental shelves and sills at the eastern and western mouths of the basin (200 and 400 m, respectively) that restrict water exchange between the basin and the open ocean. Limited influx of oxygenated water coupled with high productivity rates results in anoxic conditions in the deepest part of the basin, producing ideal conditions for the preservation of annually laminated or varved sediments (Reimers et al., 1990; Thunell et al., 1995). Prevailing southward

winds result in Ekman-induced upwelling in the basin that typically peaks during the spring to early summer months and relaxes during the fall and winter (Hendershott & Winant, 1996). Seasonal upwelling produces a wide range of $[CO_3^{2-}]$, temperature, and nutrient values, making this an ideal setting for examining the influence of each of these variables on foraminifera calcification.

2.2. Water Column In Situ and Model Carbonate Chemistry Data

Seasonal measurements of SBB carbonate chemistry parameters (DIC and Total Alkalinity, TA) collected by the California Cooperative Oceanic Fisheries Investigations (CalCOFI) (http://calcofi.org/) and monthly water column measurements (temperature, salinity, and chlorophyll) by the Plumes and Blooms Program (PnB; https://www.eri.ucsb.edu/research/groups/plumes-and-blooms) were used in this study. The in situ water column measurements were supplemented by and used for comparison of results from an SBB-run model simulation that is able to resolve carbonate system variables at a daily resolution. The use of the model results allows us to more closely compare carbonate chemistry trends to the biweekly sediment trap results rather than depending only on available seasonal in situ data.

The model-based estimates of the carbonate system variables (TA, DIC, pH, and Ω) and water column parameters (temperature, salinity, and nitrate concentration) at the site of the SBB sediment stem from the simulations described in detail by Turi et al. (2016). The model is based on the UCLA-ETH version of the Regional Oceanic Modeling System (Shchepetkin & McWilliams, 2005) and includes a nitrogen-based nutrient-phytoplankton zooplankton-detritus model (Gruber et al., 2006) that was extended with a carbon module (Gruber et al., 2012; Hauri et al., 2013). The CalCS model setup employed here has a horizontal resolution of 5 km and 34 levels in the vertical and spans the entire U.S. coast from about 30°N to 50°N and extends more than 1,300 km into the Pacific. The hindcast simulation (1979–2012) was forced at the surface with fluxes of heat and freshwater from European Centre for Medium-Range Weather Forecasts (ECMWF) ERA-Interim reanalysis (Dee et al., 2011). The boundary conditions at the lateral boundaries of the model consisted of a combination of climatological fields based on observations and time-varying anomaly fields derived from a global hindcast simulation with the NCAR CCSM3 model (Graven et al., 2012).

The evaluation of the model simulated pH and $\Omega_{aragonite}$ with observations revealed that the model is capturing the large-scale offshore and depth gradients very well but that it has a bias in the nearshore regions north of Point Conception (Hauri et al., 2013). Owing to the limited in situ measurements from the SBB, no assessment by the model creators was undertaken for our portion of the California Current Ecosystem; however, a comparison with a 6-year continuous time series from Santa Monica Bay suggests large biases in the upper ocean (Leinweber & Gruber, 2013). Offsets between in situ measurements and model estimates are specifically attributed to low surface ocean DIC conditions coinciding with upwelling events that result in a considerable drawdown in DIC, which is not well represented by the model.

In conducting a comparison of model simulations with available in situ data, we assess if the proposed biases exist within the simulation of the marine carbonate system at our study site. While the trends in modeled carbonate variables are in good agreement with in situ and estimates of $[CO_3^{2-}]$ measurements for the SBB (Figure 1a), the absolute values are not (Figure 1b). A comparison of in situ sea surface $[CO_{32-}]$ measured seasonally by CalCOFI and discontinuously by the Plumes and Blooms from 2007–2010 (that do not overlap with our sediment trap B/Ca time series) to coeval daily values estimated by the model indicates a nearly identical offset in $[CO_{32-}]$ and $\Omega_{calcite}$ in comparison to the two in situ time series ($[CO_{32-}]$ shown in Figure 1a). A long-term comparison of $\Omega_{calcite}$ values calculated from the CalCOFI time series from 2009–2015 indicates a relatively consistent offset, with the model simulating lower pH, $[CO_3^{2-}]$ and $\Omega_{calcite}$ values compared to in situ water column measurements ($\Omega_{calcite}$ shown in Figure 1b). For the period when there are available in situ measurements of carbonate system variables that overlap with modeled data sets (2007–2015), the mean offset between measured and modeled data was used to correct simulated model values of TA, pH, $[CO_3^{2-}]$, and Ω.

2.3. Sediment Trap Sample Collection

Planktonic foraminifera (*N. dutertrei*, *N. incompta*, and *G. bulloides*) used in this study were collected as part of an ongoing sediment trap time series in the center of the SBB (34°14′N, 120°02'W, ~580-m water depth; Thunell et al., 1995, 2007; Thunell, 1998). McLean Mark VII-W automated sediment traps equipped with 0.5-m^2 funnel openings were deployed for 6-month periods, continuously collecting samples on a
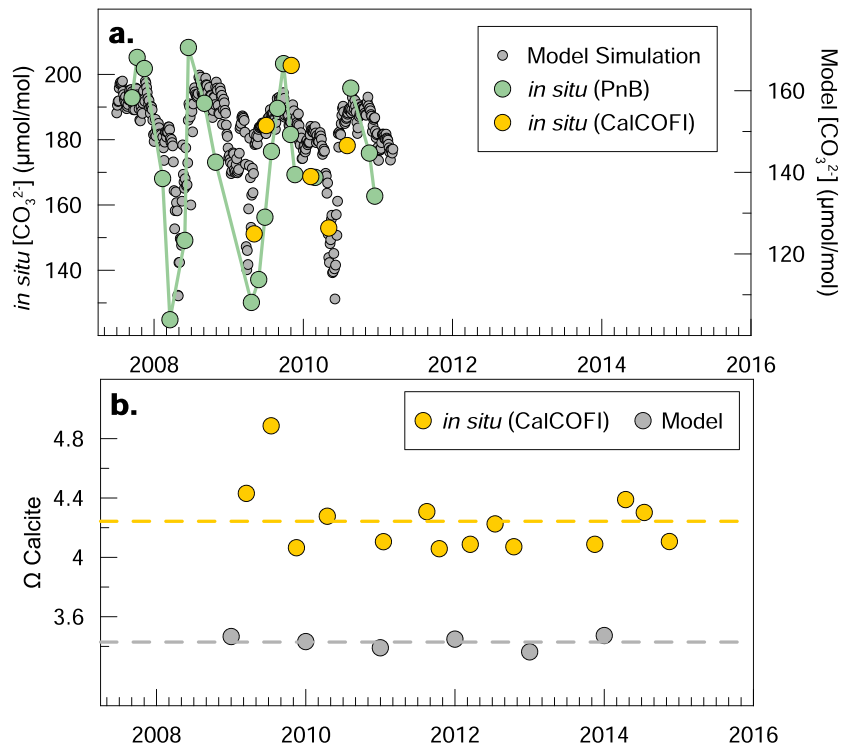
Figure 1. The upper panel (a) shows a comparison between in situ (CalCOFI and PnB) compared to coeval model hindcast estimates of $[CO_3^{2-}]$. Note that the modeled data are plotted on a unique y axis to illustrate the alignment of the carbonate system trends despite offsets in absolute values. The lower panel (b) shows the absolute value offset observed between in situ and model simulations of the carbonate system variable $\Omega_{calcite}$. Using the average offset determined from these time series comparisons, a correction was made to the model simulation values of Total Alkalinity, DIC, $[CO_3^{2-}]$ and Ω used for comparison with our B/Ca analysis.

biweekly basis. Of the two sediment traps on the mooring (top trap: 150 and bottom trap: 480-m water depth), we primarily used samples collected by the upper trap for the main analyses presented in this study; however, some bottom trap samples that were preserved in sodium borate were used in trace element cleaning methodology tests conducted as a part of this study (Text S1 in the supporting information). Sample bottles were buffered and poisoned with a sodium azide solution prior to deployment. Recovered sediments have historically been split and archived using a sodium borate buffered solution; however, the main sample suite (2015–2018; top trap) used for boron analyses in this study was never exposed to the sodium borate buffer solution and was instead split using unbuffered deionized water in order to prevent boron contamination prior to trace element analyses. Bulk sediment samples were washed over a 125-μm sieve, and the >125-μm fraction was dried in a 40 °C oven.

2.4. Planktonic Foraminifera Sample Preparation

Each dried sediment sample was processed through a series of metal mesh sieves to separate foraminifera into discrete size fractions (150–250, 250–355, 355–425, and >425 μm). Using a stereo microscope, individual foraminifera shells were handpicked from each sample and carefully selected to ensure minimal or no signs of diagenetic alteration or authigenic mineral deposits. Due to the considerable size differences across the study species, not all species were found across the size fractions. When abundant sample material was available within a sample size fraction, duplicate foraminifera samples were prepared for trace element analysis. A minimum of 100 μg of foraminiferal calcite was required for B/Ca analyses, but samples generally consisted of 150- to 200-μg calcite. After recording the weight of each sample population, the shells were loaded into 1.5-ml boron-free 10% HCL cleaned polypropylene centrifuge tubes for cleaning.

Foraminifera were then chemically cleaned following the general methodology of Boyle and Keigwin (1985) in a boron-free laboratory using mannitol-distilled MQ water and reagents and standard solutions stored in

Teflon® bottles to minimize contamination. Individual shells were gently cracked open within centrifuge tubes using a pipette tip. Clay particulates adsorbed to the surface of the cracked shells were removed in a series of mannitol-distilled MQ (three times) and methanol (two times) rinses, each followed by a brief (60 s) sonication. A subsequent reductive cleaning treatment using an optima grade NH_4OH buffered 4% hydrazine solution was applied to each sample before they were placed in a 30-min hot water bath with intermittent sonications (every 2 min). To remove any remnant organic matter, samples underwent an oxidative treatment in which a solution of 1% H_2O_2 in 0.1 N NaOH was added to each sample before being placed in a hot water bath for 10 min, with intermittent sonications every 5 min. The oxidative treatment was particularly important for our sample set, as sediment trap collections yield organic-rich sediments. Following this step, cleaned calcite fragments were transferred to a new set of boron-free HCL-refluxed polypropylene microcentrifuge tubes in which cleaned samples were briefly leached with 0.001-M quartz distilled HNO_3 to remove any mobilized contaminants.

2.5. HR-ICP-MS Elemental Analysis

Sample trace element concentrations were measured using a Thermo Element II HR-ICP-MS at the University of South Carolina's Center for Elemental Mass Spectrometry Laboratory adopting the methodology of Misra et al. (2014). Low concentrations of boron in foraminiferal calcite and high instrumental blank were addressed by using an acid matrix of 0.1 N HNO_3 + 0.06 N HF for both samples and standards. The use of HF limits the adsorption of boron onto instrumental surfaces and reduces instrumental boron blanks. A specialized Teflon spray chamber, platinum injector and platinum sample (normal), and skimmer (H) cones were used for boron analyses due to their resistance to degradation as a result of prolonged contact with HF. A lower concentration of HF is used in our study relative to Misra et al. (2014; 0.1N HNO_3 + 0.3N HF), due to the instability of the high calcium concentration samples analyzed in our study. Tests of an acid matrix containing 0.3N HF increased the variability of Ca concentrations for repeated measurements of a multielement solution standard due to the reaction of HF with Ca and the formation of calcium fluoride precipitates in solution. Results from Misra et al. (2014) indicate that an acid matrix containing 0.06 N HF is sufficient for the removal of residual boron, preventing contamination by previous samples and maintaining a low boron blank.

After sample dissolution in the 0.1 N HNO_3 + 0.06 N HF acid matrix, a small aliquot of the digestion was used to determine the calcium concentration of each sample. Sample solutions were matrix matched with standards (Yu et al., 2005) to minimize analytical error resulting from matrix effects, and measured B/Ca ratios are dependent on calcium concentrations due to matrix-induced mass-related discrimination (Misra et al., 2014; Yu et al., 2005). After preliminary measurement of sample calcium concentrations, each sample was uniquely diluted to meet the target calcium concentration of 20 ppm for our *G. bulloides* and *N. incompta* foraminiferal analyses. Due to the lower boron content of *N. dutertrei* (~40–55 μmol/mol) relative to *G. bulloides* (~60–100 μmol/mol) and *N. incompta* (~50–80 μmol/mol), we chose to dilute *N. dutertrei* samples to a higher calcium concentration of 30 ppm to ensure a robust sample boron signal well above the instrumental blank.

A five-point standard calibration was used to estimate the element/calcium ratios of samples. The contribution of boron and magnesium from single-element stock solutions was monitored using a standard (Standard-0) that consisted of only the mixed acid matrix and Ca. The multielement standard calibration was blank corrected for the boron and magnesium concentrations measured in standard-0, typically accounting for 20% and 1% of the total boron and magnesium blanks, respectively. Repeated measurements of a standard with Mg/Ca of 3.5 mmol/mol and B/Ca of 124.5 μmol/mol had reproducibility of ±0.02 (±0.61%) and ±1.7 (±1.39%), respectively. Repeat measurements of one of the multielement standards (that most closely matched the geochemistry of the run samples) were measured between every three samples to monitor instrumental drift and apply drift corrections as needed. Procedural blanks measured at the beginning of the first analytical run for a given sample batch were within error of instrumental blanks. While the instrumental boron blank accounts on average for 20% of the boron measured for a given sample, the standard deviation of blanks measured during a single analytical run is consistent with standard deviations of repeat measurements of a standard multielement solution representing only 5% of the blank value.

To assess the analytical precision of our boron method for calcite matrix samples, we created a homogenized foraminifera standard. The foraminifera (*Globorotalia menardii*) used to create our standard were taken

from a single sediment trap sample representative of a 2-week sampling period from the Cariaco Basin Time Series. A large foraminiferal bloom resulted in a huge accumulation of foraminifera, ideal for creating a large foraminifera-based standard. Approximately 10 mg of *G. menardii* was cleaned in 2-mg batches following the cleaning procedure described above for sample preparation. Approximately 200-µg subsamples of crushed and homogenized foraminifera was used for replicate measurements and resulted in excellent reproducibility of both B/Ca (72.5 ± 0.17 1SD mmol/mol) and Mg/Ca (2.55 ± 0.17 1SD mmol/mol) measurements (Figure S4).

2.6. Laser Ablation-ICP-MS Analysis

The laser ablation inductively coupled plasma-mass spectrometry (LA-ICP-MS) at the University of Cambridge's Department of Earth Science was used to measure trace element ratios of individual foraminiferal shells. Individual analyses were conducted based on the inconclusive results of the *G. bulloides* population B/Ca time series measured by HR-ICP-MS. In order to better evaluate intrasample variability and the possible presence of cryptic species, individual analyses by LA-ICP-MS were employed. A population of 49 *G. bulloides* shells from the top trap collection of January 2014 was used for the LA-ICP-MS analysis. This particular trap sample was selected based on previous sediment trap cryptic species work in the SBB that indicated an increased abundance of a cryptic *G. bulloides* species during cool periods such as peak upwelling and winter months (Darling et al., 2003; Osborne et al., 2016; Sautter & Thunell, 1991). Prior to shipment from the University of South Carolina to the University of Cambridge, the 49 individuals were individually weighed and photographed following the area density methodology of Osborne et al. (2016). Photographs were analyzed for an estimated shell diameter and 2-D surface area and used with individual shell weights to estimate area density (a proxy for shell thickness; Marshall et al., 2013; Osborne et al., 2016). Following these morphometric analyses, a total of 33 *G. bulloides* shells arrived intact at the University of Cambridge and was analyzed for B/Ca and Mg/Ca composition.

The LA-ICP-MS system employs an Analyte G2 excimer laser (Teledyne Photon Machines Inc) coupled with a Thermo i-CapQ ICPMS to measure trace metal profiles through foraminiferal shell walls. Sample preparation and analyses were carried out following protocols discussed in Eggins et al. (2003) and Sadekov et al. (2008). The horizontal and vertical resolution of the technique was optimized by ablating small diameter spots (30×30 µm) at four laser pulses per second and 1.6-J/cm^2 laser fluence. Between three and five profiles were generated for each foraminiferal shell (i.e., one profile for each chamber). The ICP-MS is optimized by using NIST610 reference glass material for maximum sensitivity across Li-Sr mass range and maintaining ThO/Th <0.5% and Th/U ratio ~1. The isotopes 11B, 24Mg, 32S, 43Ca, 44Ca, 55Mn, 63Cu, 66Zn, 88Sr, 138Ba, and 27Al were measured during each depth profile analysis, which required only 20–50 s to acquire. Data reduction involved initial screening of spectra for outliers, subtraction of the mean background intensities (measured with the laser turned off) from the analyzed isotope intensities, internal standardization to 43Ca, and external standardization using the NIST-SRM610 glass reference material. The signals of Al, Mn, Zn, Cu, and Ba were used to distinguish surface contamination from foraminiferal calcite following Sadekov et al. (2008). The in-house calcitic standard eBlue was used to monitor long-term B/Ca and Mg/Ca reproducibility, which was 252 ± 8 and 3.63 ± 0.17 mmol/mol, respectively.

3. Results and Discussion

3.1. *Neogloboquadrina* Population HR-ICP-MS B/Ca

A total of 26 sediment trap samples spanning October 2013 to October 2014 was processed to generate a nearly continuous yearlong time series of B/Ca ratios for both nonspinose *Neogloboquadrina* species (*N. dutertrei* (Figure 2a and Table 1) and *N. incompta* (Figure 2b and Table 2)). However, Ekman-induced upwelling that begins in February and persists through July resulted in an overall lower flux of both species during this period and presents some temporal gaps in the B/Ca time series. When sufficient numbers of foraminifera were present in a sediment trap sample, multiple measurements were made for varying size fractions (11 out of 19 *N. dutertrei* samples and 3 out of 17 *N. incompta* samples) in order to evaluate size effects on B/Ca. The greater size range and overall larger individual size and mass of *N. dutertrei* allowed for a greater number of size fraction measurements within a single sediment trap sample. In contrast, the lower abundance and smaller individual size (generally restricted to the 150- to 255-µm size fraction) of *N. incompta* hampered sample replication for the majority of the time series.
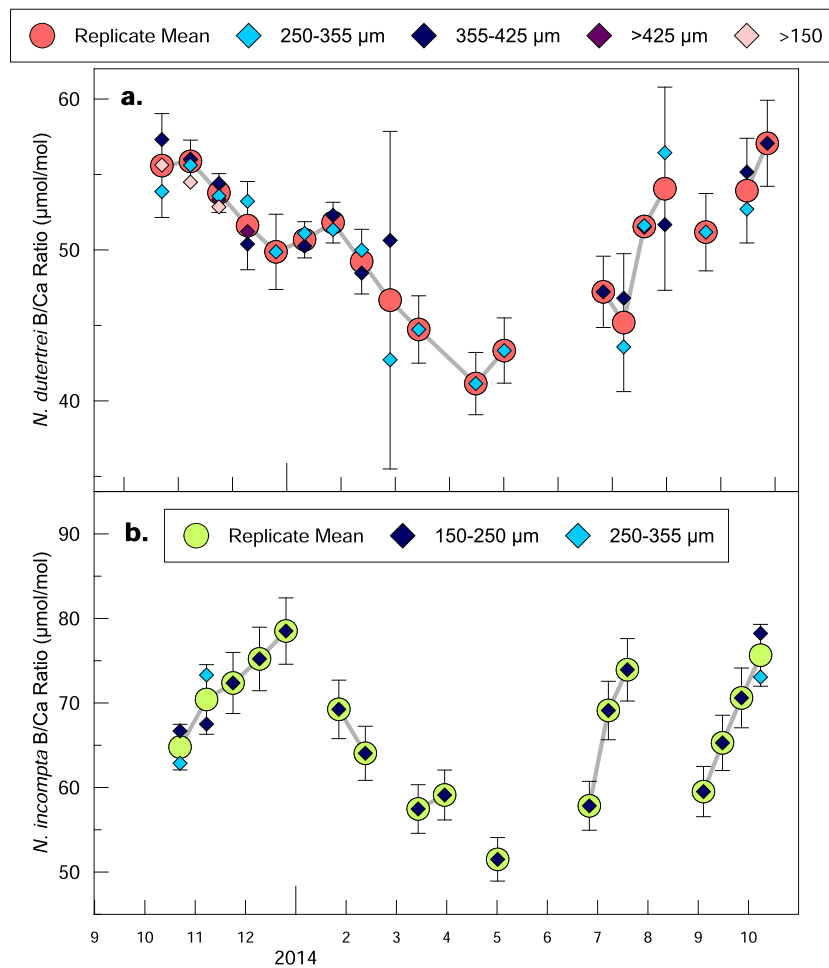
Figure 2. October 2013 to October 2014 sediment trap time series of *Neogloboquadina* B/Ca. Error bars on sample means indicate 2-sigma errors based on the multiple measurements made for a given sample. When only a single measurement was made, error bars represent the fully propagated analytical error associated with each measurement. The upper panel (a) shows the time series of *N. dutertrei* B/Ca measurements from 19 sediment trap samples. Multiple measurements were made for a single sediment trap sample when *N. dutertrei* was present over multiple size fractions in order to evaluate size effects of B/Ca. For several samples, measurements were made without restricting size fraction (>150 μm) to compare to size fraction restricted measurements. For 7 of the 19 sediment trap samples, only a single B/Ca measurement was made within a single size fraction due to limited sample material. The lower panel (b) shows the time series of *N. incompta* B/Ca measurements from 17 sediment trap samples. Multiple measurements were made for a single sediment trap sample when *N. incompta* was present over both the 150- to 250- and 250- to 355-μm size fractions in order to evaluate size effects of B/Ca. *N. incompta* was generally found in greater abundance in the 150–250 μm size fraction, therefore only limited number (three) of sediment trap samples allowed for measurements to additionally be made for the 250–355 μm size fraction.

B/Ca results for the *Neogloboquadina* species indicate that *N. incompta* (~50–80 μmol/mol) incorporates more boron relative to *N. dutertrei* (40–55 μmol/mol) and has roughly twice as large of a boron signal response to seasonal changes in ocean conditions that are observed in our time series (Figure 2). These results demonstrate the species-specific differences in the incorporation rate of boron into biogenic calcite of foraminifera. This is not surprising, as previous culture results have already clearly demonstrated species-specific B/Ca offsets between planktonic foraminifera (*G. ruber*, *G. sacculifer*, and *O. universa*) grown in identical seawater composition (Allen et al., 2011, 2012).

The multiple size fraction measurements made for a given sediment trap sample indicate that both species generally yield B/Ca ratios within error, regardless of shell size (Figure 2). This differs from previous studies of some dinoflagellate symbiont-bearing foraminifera species that demonstrated that photosynthetic activity of symbionts results in poor agreement of B/Ca measurements across size fractions for a single sampling

period (Babila et al., 2014; Salmon et al., 2016). This result for *N. dutertrei* is particularly interesting due to the fact that this species does in fact harbor symbionts. However, the dinoflagellate symbionts hosted by some spinose foraminifera typically range from 8–12 μm in size, while many nonspinose species including *N. dutertrei* host coccoid alga that are 1.5–3.5 μm in size (Fehrenbacher et al., 2011; Gastrich, 1987). Our results suggest that the relative activity of these small intracellular symbionts, which are limited by light, is much less than the large dinoflagellate symbionts that are found on extracellular spines of surface-dwelling species (Gastrich, 1987).

The large errors associated with *N. dutertrei* B/Ca measurements in March and August 2014 are the result of small sample sizes ($n = 4$, <100 μg) for each of these measurements. As with other foraminiferal geochemical analyses (δ^{18}O, Mg/Ca), ideally a large number of individuals are included in bulk measurements to reduce the noise of intersample variability (Ganssen et al., 2011; Killingley et al., 1981; Schiffelbein & Hills, 1984). While careful attention was paid to matrix matching [Ca] for our sample runs, these small samples also inherently include a greater fraction of the digested sample and therefore may also be impacted analytically by acid matrix effects. To further demonstrate that size does not affect *N. dutertrei* B/Ca ratios, measurements were made using individuals spanning all size fractions (150–425 μm) for three sampling periods (October–December 2013) when *N. dutertrei* were highly abundant. Broad size fraction samples produced B/Ca values that were within error of restricted size fraction measurements, further demonstrating that neither size nor the presence of symbionts in *N. dutertrei* influences the boron signal of this species.

3.2. Comparison of *Neogloboquadrina* B/Ca to Ambient Carbonate Chemistry

We compare B/Ca ratios of each species to modeled water column data to assess the relationship between shell geochemistry, seawater carbonate chemistry, and other hydrographic variables. Previous studies have shown that it is important to use water column properties from the depth of calcification in order to establish the best relationship between shell geochemistry and seawater conditions. A study from the Southern California Bight indicates that the δ^{13}C of *N. incompta* (also referred to as *N. pachyderma* (right coiling)) and *N. dutertrei* from this region is in equilibrium with δ^{13}C at thermocline or subthermocline depths, which range between 25- and 40-m water depths during nonupwelling periods in SBB, when these species are most abundant (Sautter & Thunell, 1991). Equatorial Pacific Multiple Opening/Closing Net and Environmental Sensing System tows collected *N. dutertrei* from the sea surface to over 1,000 m water depth, but oxygen and carbon isotopic results indicate that *N. dutertrei* calcite is in equilibrium with seawater at ~30 m water depth (Fairbanks et al., 1982). This suggests that *N. dutertrei* produces the majority of their shell calcite at ~30-m water depth before descending through the water column during later life stages (Fairbanks et al., 1982). A study that included core top *N. incompta* δ^{18}O values from our study region determined a mean calcification depth range of 25–45 m with an average estimated calcification depth of 35-m water depth (Quintana Krupinski et al., 2017). Calcification depths for both species in the SBB were estimated using Mg/Ca-derived temperatures and comparing directly to coeval measured in situ temperature profiles from PnB CTD casts. Temperature was estimated from Mg/Ca ratios using the equations of Anand et al. (2003) for *N. dutertrei* and for mixed species. Our estimated Mg/Ca-temperatures suggest average calcification depths for *N. dutertrei* and *N. incompta* of ~30 and ~40 m, respectively, over the course of the sediment trap sampling period.

A comparison of *N. dutertrei* (30 m) and *N. incompta* (40 m) B/Ca to the respective depth modeled carbonate chemistry values (pH, $\Omega_{calcite}$ and $[CO_3^{2-}]$) indicates an excellent agreement with seasonal trends (B/Ca compared to $\Omega_{calcite}$; Figure 3). For our analysis we chose to strictly present empirical comparisons between B/Ca and carbonate chemistry values directly simulated by the model. We do not report relationships with K_D as proposed by Yu et al. (2007) and applied by others in calibration studies (e.g., Allen et al., 2011, 2012; Henehan et al., 2015; Howes et al., 2017), as the model outputs do not simulate $[B(OH)_4^-]$ nor do we have in situ measurements needed to confidently correct the model bias that must be accounted for. Further, an additional layer of uncertainty would be introduced by using these corrected values to calculate K_D; therefore, these values are not reported without our study. While this is a limitation that hinders some comparisons to previous work, the highly significant correlations observed empirically with carbonate chemistry parameters in our study provide additional support of the B/Ca proxy and shed light on boron incorporation in these relatively understudied species.
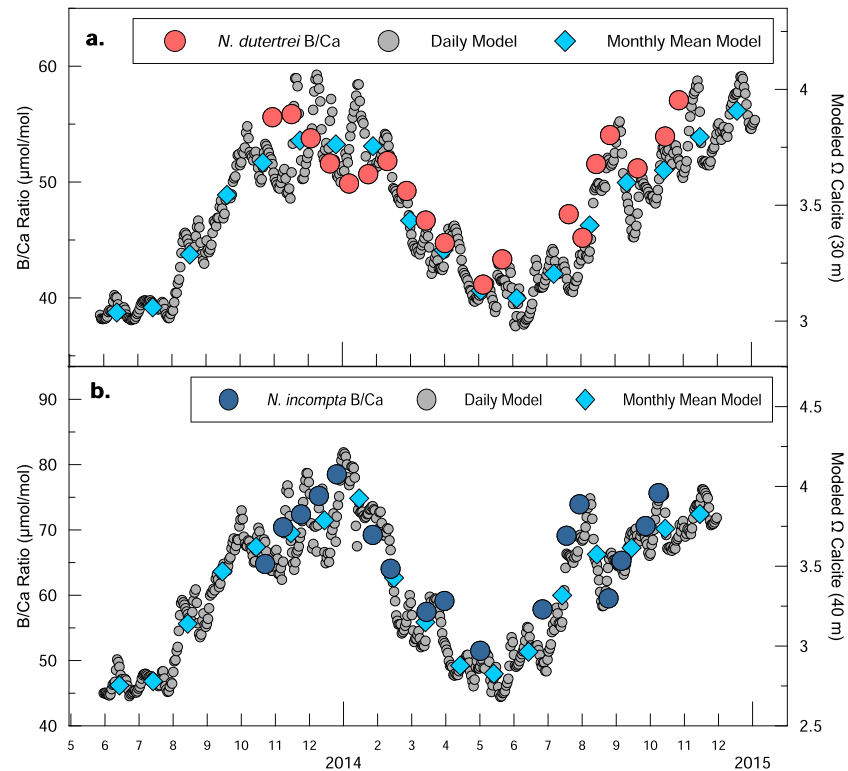
Figure 3. The upper panel (a) shows the mean replicate B/Ca ratios of *N. dutertrei* (pink circles) compared to modeled 30 m $\Omega_{calcite}$. Model data are shown here as daily (gray circles) and monthly mean (blue diamonds) values. The lower panel (b) shows the mean replicate B/Ca ratios of *N. incompta* (navy circles) compared to modeled 40 m $\Omega_{calcite}$. Model data are shown here as daily (gray circles) and monthly mean (light blue diamonds) values.

3.3. Evaluating the Controls on *Neogloboquadrina* B/Ca and Comparison to Published Results

While seasonal upwelling in the SBB provides a wide range of hydrographic conditions ideal for proxy calibration, it also results in covariation of certain hydrographic parameters. Linear regressions between the independent variables examined in this study (pH, $[CO_3^{2-}]$, $\Omega_{calcite}$, NO_3^-, temperature, and salinity) indicate collinearity between all of the variables (Figure 4). This is due to upwelling processes, which introduce subsurface waters to the surface ocean that are cool, saline, and nutrient rich due to the remineralization of organic matter at depth. Subsurface water masses that reach the sea surface during upwelling are also enriched in DIC due to remineralization, which results in naturally lower in pH, $[CO_3^{2-}]$ and $\Omega_{calcite}$ of conditions during seasonal upwelling events in our study region.

Though a positive correlation between temperature and B/Ca is observed in both species, correlations with temperature may well be spurious due to the fact that temperature and carbonate system parameters (pH, $[CO_3^{2-}]$, and $\Omega_{calcite}$) are highly correlated. A strong correlation between Mg/Ca (a temperature proxy) and B/Ca ratios for both species further illustrates the covariation of the independent variables that control shell geochemistry (*N. dutertrei* $R^2 = 0.81$, *N. incompta* $R^2 = 0.83$, Figure S5). Culture experiments indicate that temperature has a negligible effect on B/Ca in symbiont-bearing planktonic foraminifera (Allen et al., 2011, 2012; Henehan et al., 2015), and Pacific core top results for *G. bulloides* and *N. incompta* indicate that the relationship between Mg/Ca-estimated temperatures and B/Ca ratios is likely due to temperature and Ω being highly correlated (Quintana Krupinski et al., 2017). Inorganic calcite precipitation studies have also indicated negative or insignificant influence of temperature on B/Ca ratios (Mavromatisa et al., 2015; Kaczmarek et al., 2016; Uchikawa et al., 2015).

A strong negative correlation between B/Ca ratios and salinity (*N. dutertrei* $R^2 = 0.68$, $p = <0.003$ and *N. incompta* $R^2 = 0.43$, $p = <0.025$) observed in our data set differs from some previously published results for both symbiont-bearing and symbiont-barren species. Core top and culture results have reported
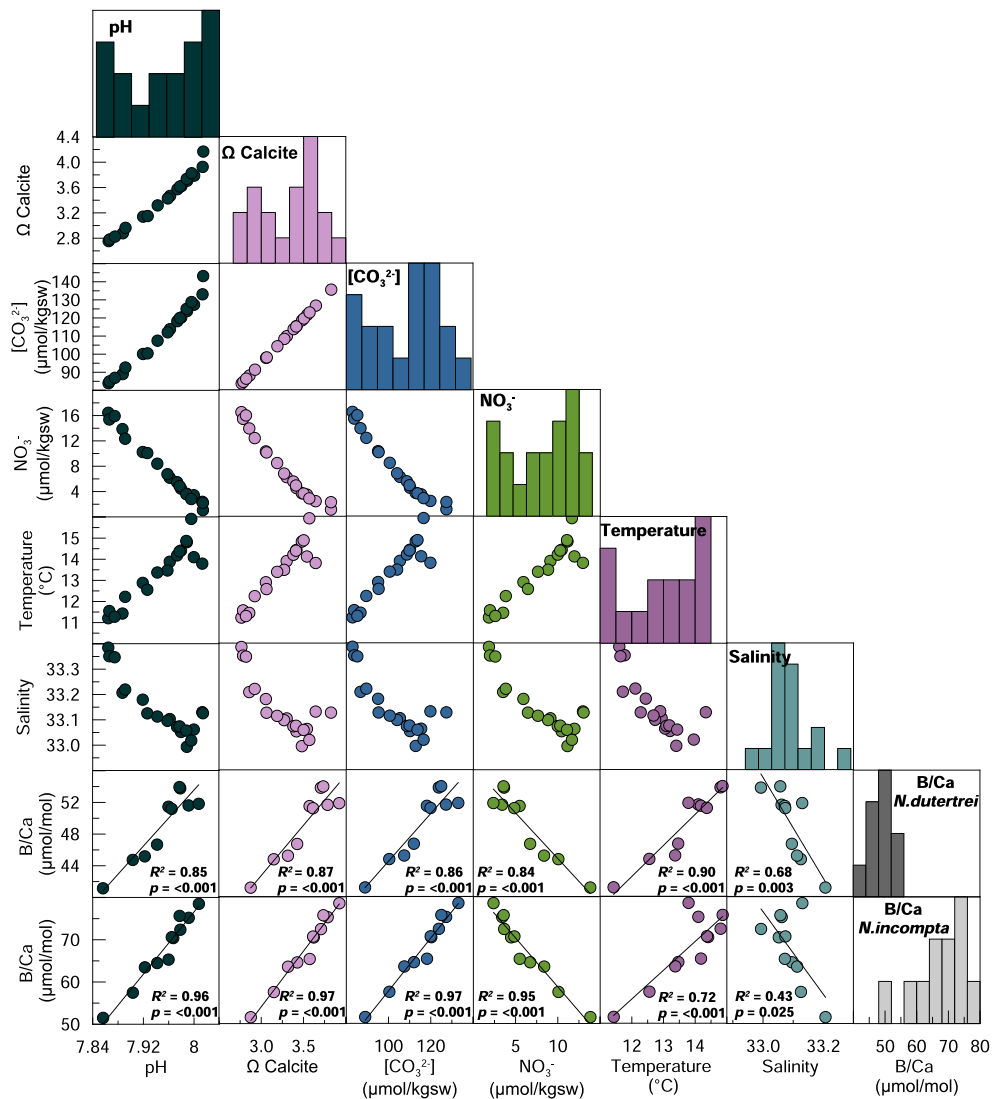
Figure 4. Matrix of linear regressions showing the relationship between the B/Ca ratios of *Neogloboquadrina* species and the monthly mean value determined for each relevant available independent variables predicted by the model simulation. Histograms are included to show range and frequency for each variable.

positive correlations with salinity (Allen et al., 2011, 2012 Quintana Krupinski et al., 2017); however, two sediment trap time series found large fluctuations in B/Ca at a site where salinity changes negligibly, suggesting a nondominant control of salinity on B/Ca (Babila et al., 2014; Salmon et al., 2016). The strongest correlation between B/Ca and salinity was reported in a global compilation of sediment trap, tow, and core top B/Ca that was supplemented with new culture results for the symbiont-bearing species *G. ruber* (white) (Henehan et al., 2015). While B/Ca-salinity correlations far outweighed the statistical contribution of carbonate chemistry on B/Ca in this study, the authors noted that a mechanistic understanding of the salinity relationship is not yet confirmed (Henehan et al., 2015). Inorganic precipitation experiments observed a modest increase in B/Ca salinity and suggested that in the presence of oxyanions in growth solutions cause surface roughening of calcium carbonate due to formation of crystallographic irregularities that could further facilitate boron incorporation (Uchikawa et al., 2017). Because the opposite sign of this relationship is revealed in our data set, we suggest that salinity, while possibly an influential variable, is overwhelmed by the carbonate chemistry influence, which we suggest is the dominant control on B/Ca in our study species. The negative relationship between B/Ca and salinity is specifically an artifact of the negative correlation between carbonate chemistry variables and
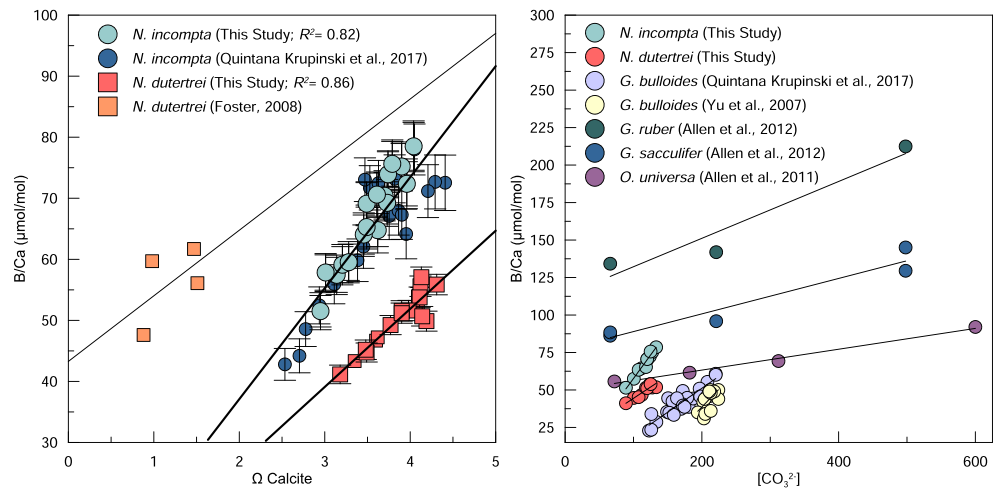
Figure 5. Regression relationships between carbonate variables ($\Omega_{calcite}$ and $[CO_3^{2-}]$) and *N. incompta* ($n = 17$) and *N. dutertrei* ($n = 19$) from this study plotted with results from a number of other studies including those that evaluated symbiont-bearing foraminifera. The slope of the *N. incompta* relationship shown here is representative of the pooled results from this study's sediment trap results and core top results for the Pacific (Quintana Krupinski et al., 2017).

salinity driven by upwelling, further suggesting that the influence of salinity is statistically less robust relative to carbonate system variables.

Nutrient concentration (measured here by nitrate (NO_3^-) rather than phosphate (PO_4^{3-}), which has been the focus of previous culture and core top studies) is also negatively correlated with B/Ca ratios in our data set (*N. dutertrei* $R^2 = 0.84$, $p = < 0.001$ and *N. incompta* $R^2 = 0.96$, $p = <0.001$). This contrasts with the considerable positive correlation observed in globally distributed core tops between *G. ruber* and $[PO_4^{3-}]$ (Henehan et al., 2015) and relatively weak but significant relationship observed in culture results that included additional symbiotic foraminifera (Allen et al., 2011, 2012). While the mechanism for this relationship has not been confirmed, inorganic precipitation experiments suggest that increasing $[PO_4^{3-}]$ results in crystallographic defects allow for increased boron incorporation into the calcite lattice, the same process described above for salinity; however, $[PO_4^{3-}]$ was not cited as a dominant control but rather a secondary control for B/Ca (Uchikawa et al., 2017). A recent culture study on *O. universa* suggested that symbiont photosynthetic rates are higher under elevated $[PO_4^{3-}]$ conditions because PO_4^{3-} is a limiting nutrient and that as a result ambient pH and B/Ca within symbiont-bearing species would be elevated (Howes et al., 2017). It was postulated that the lack of a significant correlation between *N. incompta* and $[PO_4^{3-}]$ observed in Pacific core tops was due to the lack of symbionts in this species (Quintana Krupinski et al., 2017). Due to the fact that $[NO_3^-]$ and carbonate chemistry variables are strongly negatively correlated in our study due to upwelling, it is difficult to discern the importance of $[NO_3^-]$, aside from the fact that this relationship is less statically robust. While it is unclear what role nutrient concentration plays in asymbiotic species, we suggest that it has little to no significant influence on B/Ca in our study species.

The highest correlation coefficients observed in our study are between *N. incompta* and *N. dutertrei* B/Ca and the carbonate system parameters (Figure 4). The relationships observed between B/Ca and carbonate system variables are in excellent agreement the core top results for *N. incompta* from the Pacific, which demonstrated in particular that B/Ca is most significantly correlated with $\Omega_{calcite}$ (Figure 5; Quintana Krupinski et al., 2017). A slightly higher correlation coefficient between $\Omega_{calcite}$ and B/Ca for both species, although a statistically significant difference between carbonate system variables [$\Omega_{calcite}$, pH and $[CO_3^{2-}]$], is not observed in our sediment trap data set (Figure 4). Relative to our student trap evaluation, the core top study that found the strongest relationship between *N. incompta* and $\Omega_{calcite}$ covered a wide range of hydrographic regimes where temperature and carbonate parameters were often decoupled allowing for better attribution of B/Ca signals (Quintana Krupinski et al., 2017). Inorganic precipitation studies have also indicated that carbonate chemistry conditions that correlate with higher Ω (i.e., elevated [DIC], pH, and $[Ca^{2+}]$) result

in more rapid precipitation of calcium carbonate and represent the primary controls on B/Ca (Watson, 2004; Uchikawa et al., 2015, 2017).

A comparison to previously published culture and core top calibration studies demonstrates the species-specific offsets that exist in both boron concentration and the slope of the relationship between B/Ca and carbonate chemistry parameters (Figure 5). Based on the slopes of the calibration relationships compared, symbiont-bearing species, which generally reside nearest to the sea surface, have higher B/Ca ratios relative to the deeper-dwelling, nondinoflagellate hosting or asymbiotic species. Interestingly, the slopes of the B/Ca calibrations for the large symbiont-bearing species are shallower, which could perhaps point to the symbiont mediation of ambient pH in these species.

A species-specific comparison of our B/Ca calibration results for *N. dutertrei* to those of Foster (2008) based on Pacific and Atlantic core tops shows an overlap in measured B/Ca values but a considerable offset between the Ω values used in respective calibrations. As mentioned previously, the range in measured B/Ca values for *N. incompta* and the calibration relationships found within this study are in excellent agreement with previously published core top measurements for the Pacific (Quintana Krupinski et al., 2017). A qualitative comparison of our findings to the B/Ca analysis of another symbiont-barren species, *G. truncatulinoides* (deep-dwelling species), examined from sediment trap samples collected in the North Atlantic, found highly significant correlations with shell thickness (measured by area density), which is a reported proxy for $[CO_3^{2-}]$ and directly related to Ω. However, the authors surprisingly did not find a strong correlation with carbonate parameters directly, including $[CO_3^{2-}]$, which calls into question their use of inconsistent geochemical measures ($\delta^{18}O$ and Mg/Ca) and corresponding equations to estimate and select depth-specific carbonate parameters for regressions.

Taken together, we propose that carbonate parameters, specifically the $\Omega_{calcite}$ of seawater, exert the strongest control on B/Ca ratios in *N. dutertrei* and *N. incompta* because of the mechanistic relationship between calcification rate (which in inherently related to Ω) and boron incorporation into foraminiferal calcite (e.g., Quintana Krupinski et al., 2017, Uchikawa 2017). Our results set the stage for future experiments that have the ability to identify the controls on B/Ca in isolation, more fully understand the relationships between other carbonate system variables, and improve the level of confidence of these relationships prior to application to the paleorecord. Specifically, culture studies focused on these species will be instrumental to clearly constraining independent variables in isolation and identifying what variables exert the greatest control on B/Ca in these species.

3.4. *G. bulloides* Population HR-ICP-MS B/Ca

A sediment trap time series of B/Ca ratios for the asymbiotic surface-mixed layer dwelling planktonic foraminifers species, *G. bulloides*, was also developed using the October 2013 to October 2014 samples included in the study of *Neogloboquadrina* species (Figure 6). A total of 21 sediment trap samples from this period had sufficient material to make B/Ca measurements, and a total of 18 samples yielded enough material for size fraction replicates (150–250 and 250–355 μm). Periods of upwelling resulted in an overall reduction in the flux of *G. bulloides*; therefore, a sampling gap occurs during early spring when upwelling initiates.

The B/Ca of *G. bulloides* examined in our study seasonally ranges from ~60–90 μmol/mol and is higher than the measured *N. dutertrei* B/Ca (40–55 μmol/mol) but overlaps with *N. incompta* values (50–80 μmol/mol) recorded in identical sediment trap collections, highlighting the species-specific processes that are integrated into foraminiferal B/Ca values. Our SBB *G. bulloides* values are also considerably higher than those reported for the Pacific core top study (~20–60 μmol/mol; Quintana Krupinski et al., 2017) and North Atlantic and Southern Ocean core top study (~30–50 μmol/mol; Yu et al., 2007) despite overlapping ranges in carbonate system parameters. The observed offset between Pacific core top and our sediment trap results is particularly interesting, given that the core top study includes three samples within the SBB, which returned B/Ca values of 35–41 μmol/mol. An agreeable comparison of our solution-based HR-ICP-MS B/Ca results to our individual shell LA-ICP-MS results, measured by independent laboratories, that are both well above the range reported by Quintana Krupinski et al. (2017), suggesting that analytical error is not to blame for elevated values in our time series. Additional research comparing modern and seafloor *G. bulloides*, perhaps by way of culturing, would be an important next step to reconciling this discrepancy in results, as an obvious answer is not presented within our study framework.
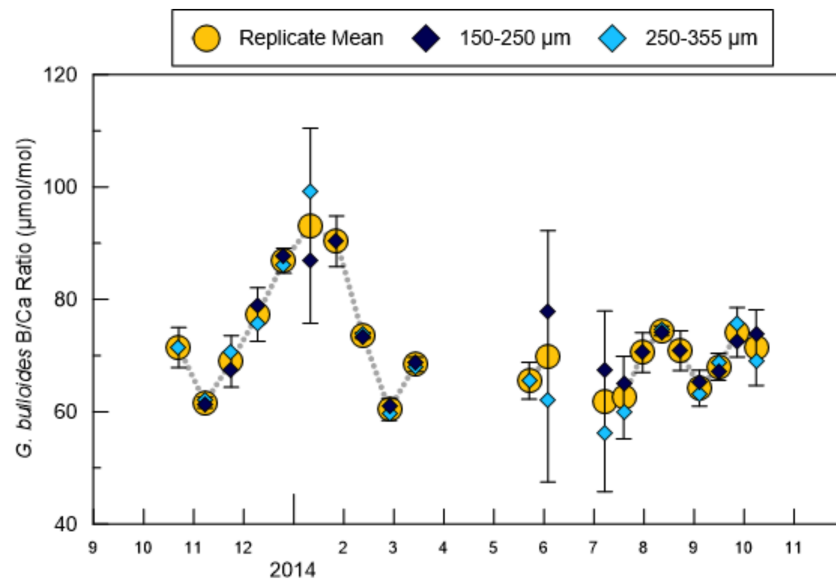
Figure 6. Time series of *G. bulloides* B/Ca measurements from sediment trap samples collected from October 2013 to October 2014. Measurements were made for the 150–250 and 250–355 μm size fractions for each sample when sufficient sample material as available. When multiple measurements were made, error bars represent the fully propagated analytical error associated with each measurement. Error bars on replicate means indicate 2-sigma errors of replicate measurements.

Overall, the *G. bulloides* B/Ca ratios duplicate well within error across size fractions with the exception of three samples during the winter and peak upwelling in early spring (Figure 6). It is important to note that, although two genetically distinct morphotypes of *G. bulloides* have previously been identified in our study region (Darling et al., 2003), we did not distinguish cryptic species within sample populations prior to pooling individuals for solution HR-ICP-MS trace element analyses. To more closely evaluate the seasonal range of B/Ca in *G. bulloides*, a series of additional sediment trap samples from December 2014 to April 2015 were analyzed to specifically cover winter months and peak upwelling periods when our results returned poor replicate measurements during the original year time series. This extended sample set demonstrates a very similar seasonal range and trend for the winter to early spring sampling months (Figure 7).
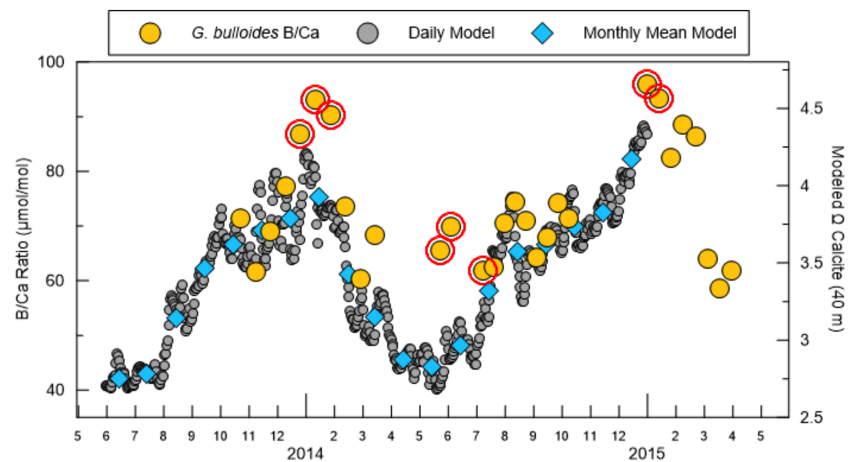

Figure 7. Mean B/Ca ratios of *Globigerinas bulloides* (yellow circles) compared to modeled 40 m $\Omega_{calcite}$. A mean calcification depth of 40 m was determined using *G. bulloides* $\delta^{18}O$ temperature estimates for a 3-year SBB sediment trap study (Osborne et al., 2016). Model data are shown here as daily (gray circles) and monthly mean (light blue diamonds) values. Red circles highlight samples that possibly include a secondary cryptic *G. bulloides* species based on environmental conditions and a comparison of B/Ca and Mg/Ca to $\Omega_{calcite}$ and temperature, respectively.

The *G. bulloides* used across this additional sampling period was not split into size fractions but was instead pooled across the 150- to 355-μm size range to ensure robust sample and population size. B/Ca ratios of *G. bulloides* were compared to modeled 40-m water column variables since the mean calcification depth for *G. bulloides* was robustly established based on a 3-year SBB sediment trap study using *G. bulloides* δ^{18}O temperature estimates (Osborne et al., 2016). A comparison of *G. bulloides* B/Ca ratios to modeled $\Omega_{calcite}$ illustrates a pattern of higher than expected B/Ca during winter and peak upwelling periods (Figure 7). A closer evaluation of Mg/Ca and δ^{18}O results from this time series also shows unexpected offsets in Mg/Ca and related temperature estimates during these same periods.

We propose that the elevated B/Ca values and increased errors observed in the *G. bulloides* time series are likely due to an increase in the abundance of a cryptic species of *G. bulloides*, which has genetically been traced to favor high-latitude environments and linked to decreased SSTs conditions in our study region (Darling et al., 2003; Osborne et al., 2016). A genetic study on foraminifera collected within the SBB reported a genotype of *G. bulloides* (type IId) was present throughout the entire annual cycle with the exception of January, when researchers recorded the additional presence of the high-latitude *G. bulloides* (type IIa) (Darling et al., 2003). Further foraminiferal genetic results for our study region replicate the findings of two distinct *G. bulloides* genotypes and also report an inability to currently visually or morphologically distinguish between lineages (Bird et al., 2017).

The earliest report of a *G. bulloides* morphotype within the Southern California Bight was based on a sediment trap study that found the "normal" morphotype in abundance throughout the year, while an "encrusted" morphotype was seasonally observed in association with cool periods such as peak upwelling and winter months (Darling et al., 2003; Osborne et al., 2016; Sautter & Thunell, 1991). Subsequent down-core studies from the SBB also indicate an increased abundance of "encrusted" individuals in the fossil record associated with glacial periods (Bemis et al., 2002; Hendy & Kennett, 2000). Since these initial visual observations of the "encrusted" morphotype were made, genetic and morphometric studies have suggested that the less abundant "encrusted" morphotype is possibly found in even higher abundances that previously thought as these morphotypes cannot always be visually identified (Darling et al., 2003; Osborne et al., 2016; Bird et al., 2017). This conundrum poses a challenge to the paleoceanographic researchers that unknowingly aggregate distinct *G. bulloides* cryptic species, particularly if they exhibit geochemical signatures like those that have been demonstrated for this species and study region (Bemis et al., 2002; Osborne et al., 2016; Sadekov et al., 2016).

Previous work on distinguishing cryptic species of *O. universa* has reported the utility of using the combination of shell weight, area and diameter (Marshall et al., 2015). By applying this methodology to our *G. bulloides* samples, we found that it is possible to clearly distinguish the two cryptic species found in the SBB by looking at a combination of morphological features (Osborne et al., 2016). While the name "encrusted" suggests that a thickly calcified exterior easily identifies the morphospecies, we find that morphometric characterization has the ability to effectively identify far more encrusted individuals than the naked eye. We applied this morphological approach to identifying cryptic species to a wintertime sediment trap sample that we suspected contained a number of the "encrusted" *G. bulloides*. We found that encrusted individuals were not only present but were actually the dominant *G. bulloides* morphotype found in this sample (Figure 8). It is important to note that an initial visual examination suggested that none of the individuals within the sample population were encrusted or thickly calcified, highlighting the importance of using the morphometric approach to discern these cryptic species.

3.5. *G. bulloides* Individual Morphometric and LA-ICP-MS B/Ca

In order to investigate whether the presence of the two *G. bulloides* morphospecies is the cause of the discrepant B/Ca results we observed, we measured individual shells of both morphospecies via LA-ICP-MS. This single shell analyses provide an opportunity to evaluate how B/Ca ratios vary across a single sample population that have been grouped based on traditional species classification. This was particularly important to resolving the mixed results from our solution-based HR-ICP-MS as these measurements were based on indiscriminant populations of *G. bulloides*. Due to the destructive nature of HR-ICP-MS analyses, the exact sample population used for our time series could not be analyzed; however, we were able to use a remaining split of a sediment trap from January 2014 (when we found encrusted *G. bulloides* to be especially abundant) for morphological and LA-ICP-MS analyses (Figure 8). This sample yielded some of the poorest replicate
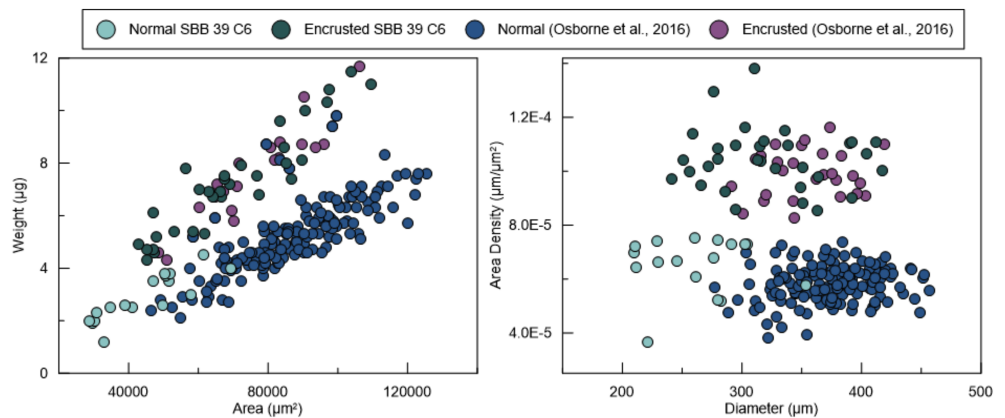
Figure 8. Morphometric analyses used to determine the presence of the normal and encrusted cryptic *Globigerina bulloides* morphospecies during the January 2014 sediment trap sampling period (SBB 39 C5). The trend in weight-area and grouping of morphospecies in the area density-diameter analyses are shown here with previously identified morphospecies groups from the SBB (Osborne et al., 2016).

B/Ca values within our time series as well as a high *G. bulloides* flux of ideal for generating a robust analysis of this time series phenomenon.

Shell morphometrics (shell weights, diameters, and 2-D surface areas) of 49 individuals were used diagnostically to identify the presence and abundance of normal and encrusted *G. bulloides* cryptic species in our sample population prior to individual analysis by LA-ICP-MS (Marshall et al., 2015; Osborne et al., 2016).
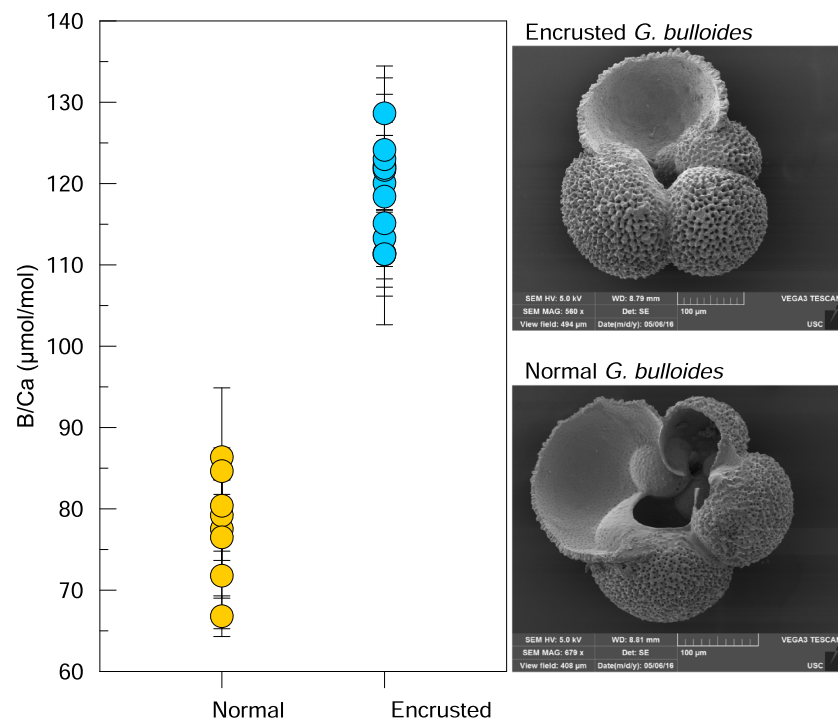

Figure 9. Individual *Globigerina bulloides* B/Ca ratios measured by LA-ICP-MS show a considerable species offset between the normal and encrusted cryptic species present in the SBB. This result shows that the less abundant "encrusted" morphotype incorporates higher concentrations of boron relative to the "normal" form that is found throughout the year in our study region. Cryptic species were determined prior to LA-ICP-MS analysis by evaluating morphometric characteristics of individual shells. Scanning electron microscope images of cracked *G. bulloides* shell show the similar appearance of external shell textures and relative difference between shell wall thicknesses, as reflected by morphometric measurements.

Morphometric results indicated that more than half of this particular sample population was composed of encrusted *G. bulloides* (Figure 8). A comparison of individual *G. bulloides* LA-ICP-MS results separated into the morphometrically classified "normal" and "encrusted" types indicate that there is in fact a significant offset in B/Ca (38 μmol/mol) between these cryptic species populations. The "encrusted" *G. bulloides* clearly incorporates higher (average: 118 μmol/mol, range: 104–128 μmol/mol) concentrations of boron relative to the "normal" *G. bulloides* (average: 79 μmol/mol, range: 67–86 μmol/mol) form (Figure 9). This difference in B/Ca between *G. bulloides* cryptic species represents a larger offset than is observed across the entire range of symbiont-bearing foraminifera (*O. universa* to *G. ruber;* Allen et al., 2011, 2012).

This B/Ca offset between cryptic spices explains higher population B/Ca ratios measured by HR-ICP-MS during periods when the "encrusted" form is typically found in higher abundance in our study region. Poor replication across samples specifically during peak upwelling and winter periods also suggests varied proportions of normal and encrusted individuals in sample populations that are presented greater offsets in population B/Ca results. Given the significantly higher B/Ca of encrusted *G. bulloides*, which are found in abundance during cooler environmental conditions, the inclusion of these individuals in down core reconstructions, for example, across glacial-interglacial transitions, has the potential to seriously hinder reconstructions based on this species.

Previous studies have reported offsets in oxygen and carbon stable isotopes for the Southern California Bight *G. bulloides* (Bemis et al., 2002; Osborne et al., 2016), and LA-ICP-MS results from the Arabian Sea revealed Mg/Ca offsets which the authors attribute to the presence of two genetically distinct *G. bulloides* morphotypes in that region (Sadekov et al., 2016). Previous work in the Pacific by Quintana Krupinski et al. (2017) observed encrusted *G. bulloides* in some core top samples and reported distinct physical and some chemical (Mg/Ca and δ^{18}O) properties relative to the normal morphospecies; however, no offset in B/Ca was reported. It is important to note that "encrusted" individuals were only visually identified, and no individual LA-ICP-MS analyses were included in this study (Quintana Krupinski et al., 2017). Interestingly, other B/Ca studies have posed the idea that mixed B/Ca results could be the result of mixing genetically distinct cryptic species within their sample populations (Henehan et al., 2015); however, this has yet to be the focus of B/Ca analyses to date.

4. Conclusions

Investigating B/Ca in nondinoflagellate hosting foraminifera presented an opportunity to evaluate the B/Ca proxy without complications such as intrashell heterogeneity, size effects, and presence of large symbionts that alter the microenvironment around the foraminifera. Our work suggests that B/Ca ratios of asymbiotic *N. incompta* and nondinoflagellate-bearing *N. dutertrei* are not influenced by shell size and have a strong potential to serve as robust carbonate system proxies. Future culturing experiments have the ability to build upon these results by developing a more robust mechanistic understanding of which carbonate system and water column variables exert control on boron incorporation for these species. In the case of *G. bulloides*, our study sheds light on the importance of identifying and distinguishing cryptic species that are often not identified in traditional species classification approaches. We observed a significant offset in the geochemistry of two cryptic species of *G. bulloides* that have previously been identified as being genetically distinct in our study region. This finding suggests that vital effects and the effects of ecological habitats can be significant (even within a foraminiferal species complex), and genotype-specific calibrations can be of great importance when developing geochemical proxies such as B/Ca. Future work is needed to assess the genetic variance between traditional species classifications in order to better understand the influence of species-specific vital effects and offsets in trace element incorporation prior to application to the fossil record.

References

Allen, K., Hönisch, B., Eggins, S., & Rosenthal, Y. (2012). Environmental controls on B/Ca in calcite tests of the tropical planktic foraminifera species *Globigerinoides ruber* and *Globigerinoides sacculifer. Earth and Planetary Science Letters*, *351-352*, 270–280.

Allen, K., Hönisch, B., Eggins, S., Yu, J., Spero, H., & Elderfield, H. (2011). Controls on boron incorporation in cultured tests of planktic foraminifera Orbulina universa. *Earth and Planetary Science Letters*, *309*, 291–301.

Anand, P., Elderﬁeld, H., & Conte, M. H. (2003). Calibration of Mg/Ca thermometry in planktonic foraminifera from a sediment tap time series. *Paleoceanography*, *18*(2), 1050. https://doi.org/10.1029/2002PA000846

Babila, T., Rosenthal, Y., & Conte, M. H. (2014). Evaluation of the biogeochemical controls on B/Ca of *Globigerinoides ruber* white from the Ocean Flux Program, Bermuda. *Earth and Planetary Science Letters*, *404*, 67–76.

Bemis, B. E., Spero, H. J., & Thunell, R. C. (2002). Using species-specific paleotemperature equations with foraminifera: A case study in the Southern California Bight. *Marine Micropaleontology*, *46*, 405–430.

Bird, C., Darling, K. F., Russell, A. D., Davis, C. V., Fehrenbacher, J., Free, A., et al. (2017). Cyanobacterial endobionts within a major marine planktonic calcifier (*Globigerina bulloides*, Foraminifera) revealed by 16S rRNA metabarcoding. *Biogeosciences*, *14*, 1–20. https://doi.org/10.5194/bg-14-1-2017

Boyle, E. A., & Keigwin, L. D. (1985). Comparison of Atlantic and Pacific paleochemical records for the last 215,000 years: Changes in deep ocean circulation and chemical inventories. *Earth and Planetary Science Letters*, *76*, 135–150. https://doi.org/10.1016/0012-821X(85)90154-2

Branson, O., Kaczmarek, K., Redfern, S. A. T., Misra, S., Langer, G., Tyliszczak, T., Bijma, J., & Elderfield, H. (2015). The coordination and distribution of B in foraminiferal calcite. *Earth and Planetary Science Letters*, *416*, 67–72. Dai, Y., Yu, J., & Johnstone, H. J. H. (2016). Distinct responses of planktonic foraminiferal B/Ca to dissolution on seafloor. *Geochemistry, Geophysics, Geosystems*, *17*, 1339–1348. https://doi.org/10.1002/2015GC006199

Darling, K. F., Kucera, M., Wade, C. M., von Langen, P., & Pak, D. (2003). Seasonal occurrence of genetic types of planktonic foraminiferal morphospecies in the Santa Barbara Channel. *Paleoceanography*, *18*(2), 1032. https://doi.org/10.1029/2001PA000723

Dee, D. P., Uppala, S. M., Simmons, A. J., Berrisford, P., Poli, P., Kobayashi, S., et al. (2011). The ERA-Interim reanalysis: Configuration and performance of the data assimilation system. *Quarterly Journal of the Royal Meteorological Society*, *137*(656), 553–597. https://doi.org/10.1002/qj.828

Eggins, S., De, D. P., & Marshall, J. (2003). Mg/Ca variation in planktonic foraminifera tests: Implications for reconstructing palaeo-sea-water temperature and habitat migration. *Earth Planetary Science Letters*, *212*(3-4), 291–306.

Eggins, S., Sadekov, A. Y., & De Deckker, P. (2004). Modulation and daily banding of Mg/Ca in Orbulina universa tests by symbiont photosynthesis and respiration: A complication for seawater thermometry? *Earth Planetary Science Letters*, *225*, 411–419.

Elderfield, H., Vautravers, M., & Cooper, M. (2002). The relationship between shell size and Mg/Ca, Sr/Ca, d18O, and d13C of species of planktonic foraminifera. *Geochemistry, Geophysics, Geosystems*, *3*(8), 1052. https://doi.org/10.1029/2001GC000194

Fairbanks, R. G., Sverdlove, M., Free, R., Wiebe, P. H., & Bé, A. W. H. (1982). Vertical distribution and isotopic fractionation of living planktonic foraminifera from the Panama Basin. *Nature*, *298*, 841–844. https://doi.org/10.1038/298841a0

Fehrenbacher, J. S., Spero, H. J. & Russell, A. D. (2011). Observations of living non-spinose planktonic foraminifers *Neogloboquadrina dutertrei* and *N. pachyder*ma from specimens grown in culture, *AGU Fall Meeting 2011*, Abstract #PP41A-1724.

Fehrenbacher, J. S., Spero, H. J., Russell, A. D., Vetter, L., & Eggins, S. (2015). Optimizing LA-ICP-MS analytical procedures for elemental depth profiling of foraminifera shells. *Chemical Geology*, *407-408*, 2–9.

Foster, G. L. (2008). Seawater pH, pCO$_2$ and [CO$_3^{2-}$] variations in the Caribbean Sea over the last 130kyr: A boron isotope and B/Ca study of planktonic foraminifera. *Earth and Planetary Science Letters*, *271*, 254–266. https://doi.org/10.1016/j.epsl.2008.04.015

Ganssen, G. M., Peeters, F. J. C., Metcalfe, B., Anand, P., Jung, S. J. A., Kroon, D., & Brummer, G.-J. (2011). Quantifying sea surface temperature ranges of the Arabian Sea for the past 2000 years. *Climate of the Past*, *7*, 1337–1349.

Gastrich, M. D. (1987). Ultrastructure of a new intracellular symbiotic alga found within planktonic foraminifera1. *Journal of Phycology*, *23*(4), 623–632.

Graven, H. D., Gruber, N., Key, R., Khatiwala, S., & Giraud, X. (2012). Changing controls on oceanic radiocarbon: New insights on shallow-to-deep ocean exchange and anthropogenic CO$_2$ uptake. *Journal of Geophysical Research*, *117*, C10005. https://doi.org/10.1029/2012JC008074

Gruber, N., Frenzel, H., Doney, S. C., Marchesiello, P., McWilliams, J. C., Moisan, J. R., Oram, J. J., Plattner, G.-K., & Stolzenbach, K. D. (2006). Eddy-resolving simulation of plankton ecosystem dynamics in the California current system. *Deep-Sea Research I*, *53*, 1483–1516. Gruber, N., Hauri, C., Lachkar, Z., Loher, D., Frölicher, T. L., & Plattner, G. (2012). Rapid progression of ocean acidification in the california current system. *Science*, *337*(6091), 220–223. https://doi.org/10.1126/science.1216773

Hauri, C., Grube, N., Vogt, M., Doney, S. C., Feely, R. A., Lachkar, Z., et al. (2013). Spatiotemporal variability and long-term trends of ocean acidification in the California Current System. *Biogeosciences*, *10*, 193–216.

Haynes, L. L., Honisch, B., Dyes, K. A., Holland, K., Rosenthal, Y., Fish, C. R., et al. (2017). Calibration of the B/Ca proxy in the planktonic foraminifer *Orbulina universa* to Paleocene seawater conditions. *Paleoceanography*, *32*, 580–599. https://doi.org/10.1002/2016PA003069

Hemming, N. G., & Hanson, G. N. (1992). Boron isotopic composition and concentration in modern marine carbonates. *Geochimica et Cosmochimica Acta*, *56*, 537–543.

Hendershott, M., & Winant, C. (1996). Surface circulation in the Santa Barbara Channel. *Oceanography*, *9*, 114–121.

Hendy, I. L., & Kennett, J. P. (2000). Dansgaard-Oeschger cycles and the California Current System: Planktonic foraminiferal response to rapid climate change in Santa Barbara Basin, Ocean Drilling Program hole 893A. *Paleoceanography*, *15*, 30–42.

Henehan, M. J., Foster, G. L., Rae, J. W. B., Prentice, K. C., Erez, J., Bostock, H. C., et al. (2015). Evaluating the utility of B/Ca ratios in planktonic foraminifera as a proxy for the carbonate system: A case study of *Globigerinoides ruber*. *Geochemistry, Geophysics, Geosystems*, *16*(4), 1052–1069. https://doi.org/10.1002/2014GC005514

Holland, K., Eggins, S. M., Honish, B., Haynes, L. L., & Branson, O. (2017). Calcification rate and shell chemistry response of the planktonic foraminifer *Orbulina universa* to changes in microenvironment seawater carbonate chemistry. *Earth and Planetary Science Letters*, *464*, 124–134.

Howes, E. L., Kaczmarek, K., Raitzsch, M., Mewes, A., Bijima, N., Horn, I., et al. (2017). Decoupled carbonate chemistry controls on the incorporation of boron into *Orbulina universa*. *Biogeosciences*, *14*, 415–430. https://doi.org/10.5194/bg-14-415-2017

Kaczmarek, K., Nehrke, G., Misra, S., Bijma, J., & Elderfield, H. (2016). Investigating the effects of growth rate 910 and temperature on the B/Ca ratio and δ11B during inorganic calcite formation. *Chemical Geology*, *421*, 81–92. https://doi.org/10.1016/j.chemgeo.2015.12.002

Killingley, J. S., Johnson, R. F., & Berger, W. H. (1981). Oxygen and carbon isotopes of individual shells of planktonic foraminifera from Ontong-Java Plateau, Equatorial Pacific. *Palaeogeography, Palaeoecology, Palaeoclimatology*, *33*, 193–204.

Leinweber, A., & Gruber, N. (2013). Variability and trends of ocean acidification in the Southern California current system: A time series from Santa Monica Bay. *Journal of Geophysical Research: Oceans*, *118*, 3622–3633. https://doi.org/10.1002/jgrc.20259

Marshall, B. J., Thunell, R., Hennehan, M., Astor, Y., & Wejnert, K. (2013). Planktonic foraminiferal area density as a proxy for carbonate ion concentration: A calibration study using the Cariaco Basin ocean time series. *Paleoceanography*, *28*, 1–14. https://doi.org/10.1002/palo.20034

Marshall, B. J., Thunell, R. C., Spero, H. J., Henehan, M. J., Lorenzoni, L., & Astor, Y. (2015). Morphometric and stable isotopic differentiation of *Orbulina universa* morphotypes from the Cariaco Basin, Venezuela. *Marine Micropaleontology*, *120*, 46–64.

Mavromatisa, V., Montouillout, V., Noireaux, J., Gaillardet, J., & Schott, J. (2015). Characterization of boron incorporation and speciation in calcite and aragonite from co-precipitation experiments under controlled pH, temperature and precipitation rate. *Geochimica et Cosmochimica Acta*, *150*, 299–313. https://doi.org/10.1016/j.gca.2014.10.024

Misra, S., Greaves, M., Owen, R., Kerr, J., Elmore, A. C., & Elderfield, H. (2014). Determination of B/Ca of natural carbonates by HR-ICP-MS. *Geochemistry, Geophysics, Geosystems*, *15*(4), 1617–1628. https://doi.org/10.1002/2013GC005049

Ni, Y., Foster, G. L., Bailey, T., Elliott, T., Schmidt, D. N., Pearson, P., et al. (2007). A core top assessment of proxies for the ocean carbonate system in surface-dwelling foraminifers. *Paleoceanography*, *22*, PA3212. https://doi.org/10.1029/2006PA001337

Osborne, E. B., Thunell, R. C., Gruber, R., Felly, R. A., & Benitez-Nelson, C. R. (2019). Decadal variability in twentieth-century ocean acidification in the California Current Ecosystem. *Nature Geoscience*.

Osborne, E. B., Thunell, R. C., Marshall, B. J., Holm, J. A., Tappa, E. J., Benitez-Nelson, C., et al. (2016). Calcification of the planktonic foraminifera *Globigerina bulloides* and carbonate ion concentration: Results from the Santa Barbara Basin. *Paleoceanography*, *31*(8), 1083–1102. https://doi.org/10.1002/2016PA002933

Quintana Krupinski, N. B., Russell, A. D., Pak, D. K., & Paytan, A. (2017). Core-top calibration of B/Ca in Pacific Ocean *Neogloboquadrina incompta* and *Globigerina bulloides* as a surface water carbonate system proxy. *Earth and Planetary Science Letters*, *466*, 139–151. https://doi.org/10.1016/j.epsl.2017.03.007

Reimers, C. E., Kastern, M., & Garrison, R. E. (1990). In W. C. Burnett & S. R. Riggs (Eds.), *The role of bacteria mats in phosphate mineralization with particular reference to the Monterey Formation* (Vol. 3, pp. 300–311). Cambridge: Phosphate deposits of the world.

Ruiz-Agudo, E., Putnis, C. V., Kowacz, M., Ortega-Huertas, M., & Putnis, A. (2012). Boron incorporation into calcite during growth: Implications for the use of boron in carbonates as a pH proxy. *Earth and Planetary Science Letters*, *345-348*, 9–17.

Sadekov, A., Eggins, S. M., Deckker, P. D., & Kroon, D. (2008). Uncertainties in seawater thermometry deriving from intratest and interest Mg/Ca variability in *Globigerinoides ruber*. *Paleoceanography*, *23*, PA1215. https://doi.org/10.1029/2007PA001452

Sadekov, A. Y., Darling, K. F., Ishimura, T., Wade, C. M., Kimoto, K., Singh, A. D., et al. (2016). Geochemical imprints of genotypic variants of *Globigerina bulloides* in the Arabian Sea. *Paleoceanography*, *31*(10), 1440–1452. https://doi.org/10.1002/2016PA002947

Salmon, K. H., Anand, P., Sexton, P. F., & Conte, M. (2016). Calcification and growth processes in planktonic foraminifera complicate the use of B/Ca and U/Ca as carbonate chemistry proxies. *Earth and Planetary Science Letters*, *449*, 372–381.

Sanyal, A., Hemming, N. G., Broecker, W. S., Lea, D. W., Spero, H. J., & Hanson, G. N. (1996). Oceanic pH control on the boron isotopic composition of foraminifera: Evidence from culture experiments. *Paleoceanography*, *11*, 513–517.

Sautter, L. R., & Thunell, R. C. (1991). Seasonal variability in the $\delta^{18}O$ and $\delta^{13}C$ of planktonic foraminifera from an upwelling environment: Sediment trap results from the San Pedro Basin, Southern California Bight. *Paleoceanography*, *6*(3), 307–334.

Schiffelbein, P., & Hills, S. (1984). Direct assessment of stable isotope variability in planktonic foraminifera populations. *Palaeogeography, Palaeoclimatology, Palaeoecology*, *48*, 197–213.

Shchepetkin, A. F., & McWilliams, J. C. (2005). The regional oceanic modeling system (ROMS): A split-explicit, free-surface, topography-following-coordinate oceanic model. *Ocean Modelling*, *9*, 347–404.

Thunell, R. (1998). Particle fluxes in a coastal upwelling zone: Sediment trap results from Santa Barbara Basin, California. *Deep-Sea Research*, *45*, 1863–1884.

Thunell, R., Benitez-Nelson, C., Varela, R., Astor, Y., & Muller-Karger, F. (2007). Particulate organic carbon fluxes along upwelling-dominated continental margins: Rates and mechanisms. *Global Biogeochemical Cycles*, *21*, GB1022. https://doi.org/10.1029/2006GB002793

Thunell, R., Tappa, E., & Anderson, D. (1995). Sediment fluxes and varve formation in Santa Barbara Basin, offshore California. *Geology*, *23*, 1083–1086.

Turi, G., Lachkar, Z., Gruber, N., & Munnich, M. (2016). Climatic modulation of recent trends in ocean acidification in the California Current System. *Environmental Research Letters*, *11*. https://doi.org/10.1088/1748-9326/11/1/014007

Uchikawa, J., Harper, D. T., Penman, D. E., Zachos, J. C., & Zeebe, R. E. (2017). Influence of solution chemistry on the boron content in inorganic calcite grown in artificial seawater. *Geochimica et Cosmochimica Acta*, *2018*, 291–307.

Uchikawa, J., Penman, D. E., Zachos, J. C., & Zeebe, R. E. (2015). Experimental evidence for kinetic effects on B/Ca in synthetic calcite: Implications for potential B(OH)-4 and B(OH)3 incorporation. *Geochimica et Cosmochimica Acta*, *150*, 171–191. Watson, E. B. (2004). A conceptual model for near-surface kinetic controls on the trace-element and stable isotope composition of abiogenic calcite crystals. *Geochimica et Cosmochimica Acta*, *68*, 1473–1488. Yu, J., Day, J., Greaves, M., & Elderfield, H. (2005). Determination of multiple element/calcium ratios in foraminiferal calcite by quadrupole ICP-MS. *Geochemistry, Geophysics, Geosystems*, *6*, Q08P01. https://doi.org/10.1029/2005GC000964

Yu, J., Elderfield, H., & Honisch, B. (2007). B/Ca in planktonic foraminifera as a proxy for surface seawater pH. *Paleoceanography*, *22*, PA2202. https://doi.org/10.1029/2006PA001347

Erratum

In the originally published version of this article, there was a typographical error in the DOI of the Pangaea data set. The DOI has since been corrected and this version may be considered the authoritative version of record.